A NEW APPROACH FOR RE-ENTRY VEHICLE TRAJECTORY PLANNING AND GUIDANCE

Zhang Ran*, Li Huifeng*, Cao Xudong**
*** School of Astronautics, Beijing University of Aeronautics and Astronautics, Beijing 100191, China; ** Luoyang Optical & Electrical Development Center, Luoyang, 471009, China**
qdzhangran@163.com; lihuifeng@buaa.edu.cn; xudongcao2009@163.com

Keywords: *path constraints; trajectory planning; guidance law; re-entry vehicle*

Abstract

A new approach based on path constraint control is proposed in this paper for re-entry vehicle trajectory planning and guidance. A unified formula has been obtained which reveals the inherent characteristic of path constraints in r-V plane. And an analytical trajectory planning method with fewer parameters is developed. Dynamic inverse guidance law is designed to tracking the reference trajectory. Simulation results verify the feasibility of the approach.

1 Introduction

The flight of re-entry vehicle covers large range in a short time with hypersonic velocity. The vehicle faces severe aerodynamic heating and aerodynamic loads problems. Constraints like heating rate, dynamic pressure and aerodynamic load are strict. It brings great challenge to the re-entry guidance system which has to guide vehicle to the required states safely. The path constraints have to be satisfied to guarantee the structure integrity and crew safety [1].

The trajectory planning and optimization methods of high lifting re-entry vehicle can be classified in to two categories: predictor-corrector method and nominal trajectory method. The predictor-corrector methods integrate trajectory and cost a lot of time. To improve the algorithm convergence and speed, the searching parameters should be as few as possible. So lots of trajectory design methods used constant bank angle [2]. The nominal trajectory methods design the basic geometry profile of re-entry trajectory based on the engineering experience, and then adjust the profile using range predict formula to reach certain performance. It can avoid trajectory oscillations. The space shuttle re-entry trajectory profile was divided into five parts and fitted with different expressions to make the trajectory geometry fitting the shape of the constraint boundary as much as possible. The design parameters of fitted expression were searched to satisfy path constraints [3].

To enforce path constraint, Ref.[4] flatted the peak of heating rate and the vehicle flied with a constant heating rate during a short time. Ref.[5] divided trajectory into two parts: the first part flied with constant heating rate while the second part flied without any constraint. Ref.[6] used QEGC (Quasi-Equilibrium Glide Condition) and converted the constraints into the upper boundary of bank angle. Then the bank angle profile was designed under the upper boundary. However, the QEGC is not available in the whole flight.

Although the above trajectory planning methods have successfully satisfied path constraints, there are also some limitations in terms of fast convergence, efficiency, and versatility. Since the predictor-corrector method has to search a lot of parameters, it could not provide a systematically and effectively way to deal with path constraints. The nominal trajectory method also has to adjust a lot of parameters and usually based on engineering experience.

This paper firstly analysis the path constraints of heating rate, dynamic pressure and aerodynamic load in *r*-*V* plane. Based on the definition of these constraints, a unified analytical math formula which reflects the r and V relationship of constraint boundaries is obtained through derivation and integral. The characteristics which are very useful for re-entry trajectory of this formula are discussed. A new trajectory planning method is developed and dynamic inverse guidance law is also designed for trajectory tracking. The simulation results demonstrate the validity of the proposed methods.

2 Problem Description

2.1 Dynamic Equations

Three dimensional motion point-mass dynamics of the re-entry vehicle over a sphere rotating Earth described by dimensionless equations is used [7]. The distances are normalized by R_0, the radius of the Earth at the equator. Time is normalized by $\sqrt{(R_0/g_0)}$, where g_0 is the gravitational acceleration magnitude on the surface of the Earth. The velocities are normalized by $\sqrt{(R_0 g_0)}$.

$$
\begin{aligned}
&\dot{r} = V\sin\gamma \\
&\dot{\theta} = \frac{V\cos\gamma\sin\psi}{r\cos\phi} \\
&\dot{\phi} = \frac{V\cos\gamma\cos\psi}{r} \\
&\dot{V} = -D - \frac{\sin\gamma}{r^2} + \Omega^2 r\cos\phi(\sin\gamma\cos\phi - \cos\gamma\sin\phi\cos\psi) \\
&\dot{\gamma} = \frac{1}{V}(L\cos\sigma + (V^2 - \frac{1}{r})\frac{\cos\gamma}{r} + 2\Omega V\sin\psi\cos\phi + \\
&\Omega^2 r\cos\phi(\cos\gamma\cos\phi + \sin\gamma\cos\psi\sin\phi)) \\
&\dot{\psi} = \frac{1}{V}(\frac{L\sin\sigma}{\cos\gamma} + \frac{V^2\cos\gamma\sin\psi\tan\phi}{r} - \\
&2\Omega V(\tan\gamma\cos\psi\cos\phi - \sin\phi) + \frac{\Omega^2 r\sin\psi\sin\phi\cos\phi}{\cos\gamma})
\end{aligned}
\tag{1}
$$

2.2 Path Constraints

During re-entry flight, the vehicle is in hypersonic condition and must satisfy path constraints for safety and vehicle integrity such as heating rate, dynamic pressure and aerodynamic load constraints. These three most common path constraints in re-entry guidance will be discussed in detail in this paper.

1) Heating rate constraint

$$\dot{Q} = K_{\dot{Q}}\rho^{0.5}V^{3.15} \le \dot{Q}_{\max} \tag{2}$$

Where Q is the heating load. The constant $K_{\dot{Q}} = 2.8125\times10^{-4}$ for the specific vehicle in this paper. The allowed maximum heating rate $\dot{Q}_{\max}$ is determined by the thermal protection material and body structure. V is velocity and ρ is air stream density modeled as [8]:

$$\rho = \rho_0 e^{-\frac{R_0(r-1)}{H}} \tag{3}$$

Where H is a constant and ρ_0 is the sea level atmosphere density. The altitude $h=R_0(r-1)$, r is the normalized radial distance from the center of the Earth to the vehicle. The lower boundary of heating rate in r-V plane is:

$$h > -H\ln\left(\frac{\dot{Q}_{\max}^2}{K_{\dot{Q}}^2 V^{6.3}\rho_0}\right) \tag{4}$$

2) Dynamic pressure constraint

$$q = 0.5\rho V^2 \le q_{\max} \tag{5}$$

The allowed maximum dynamic pressure is mainly determined by body structure and thermal protection. The attitude is usually control through control surfaces. In order to guarantee the normal work of the control surfaces and avoid too large hinge moment, the constrained dynamic pressure should also consider these factors. The lower boundary of dynamic pressure in r-V plane is:

$$h > -H\ln\left(\frac{2q_{\max}}{V^2\rho_0 R_0 g_0}\right) \tag{6}$$

3) Aerodynamic load constraint

$$n = \sqrt{\left(L^2 + D^2\right)} \le n_{\max} \tag{7}$$

To simplify the following derivation, the L and D are normalized by mg. m is vehicle mass and g is gravity acceleration. The normalized lift and drag are:

$$
\begin{aligned}
L &= \frac{1}{2m}\rho V^2 S_{\text{ref}} R_0 C_L \\
D &= \frac{1}{2m}\rho V^2 S_{\text{ref}} R_0 C_D
\end{aligned}
\tag{8}
$$

S_{ref} is reference area. C_L and C_D are lift and drag coefficients. The allowed maximum load is determined by vehicle structure strength and the load range of onboard equipments. The lower boundary of aerodynamic load in r-V plane is:

$$h \ge -H\ln\left(\frac{2n_{\max}m}{\rho_0 V^2 R_0 S_{\text{ref}}\sqrt{\left(C_L{}^2 + C_D{}^2\right)}}\right) \tag{9}$$

The entry trajectory terminates at some distance from landing site where the guidance is handed over to the TAEM (terminal area energy management).

3 Re-entry Corridor

Re-entry corridor is determined by heating rate, dynamic pressure and aerodynamic load constraints. The space shuttle used drag acceleration and velocity to describe the corridor (D-V plane). It is because the navigation technique could not provide accurate information of velocity and altitude at that time. Another reason is that through tracking drag acceleration profile, the velocity could be controlled with small error at the condition of disturbance and uncertainties. As the development of navigation technique, the high-precision navigation becomes possible and the altitude and velocity are used (r-V plane) to describe the corridor. Actually, the D-V plane corridor and r-V plane corridor are one to one mapped. Here we use r-V plane to describe the corridor.

Different from iteration method or complicated analytic equations, here we proposed a laconic formula to describe the re-entry corridor.

Differentiating Eqs.(2), (5), and (7)with respect to V:

$$\frac{\mathrm{d}\dot{Q}}{\mathrm{d}V}=\frac{\mathrm{d}\left(K_{\dot{Q}}\sqrt{\rho}V^{3.15}\right)}{\mathrm{d}V} \tag{10}$$

$$=K_{\dot{Q}}(0.5\rho^{-0.5}V^{3.15}\frac{\mathrm{d}\rho}{\mathrm{d}V}+3.15\rho^{0.5}V^{2.15})$$

$$\frac{\mathrm{d}q}{\mathrm{d}V}=\frac{\mathrm{d}\left(0.5\rho V^{2}\right)}{\mathrm{d}V} \tag{11}$$

$$=0.5V^{2}\frac{\mathrm{d}\rho}{\mathrm{d}V}+\rho V$$

$$\frac{\mathrm{d}n}{\mathrm{d}V}=\frac{\mathrm{d}\left(\sqrt{L^2+D^2}\right)}{\mathrm{d}V} \tag{12}$$

$$=\frac{1}{n}(L\frac{\mathrm{d}L}{\mathrm{d}V}+D\frac{\mathrm{d}D}{\mathrm{d}V})$$

Where

$$\frac{\mathrm{d}\rho}{\mathrm{d}V}=-\rho\frac{R_0}{H}\frac{\mathrm{d}r}{\mathrm{d}V} \tag{13}$$

$$\begin{aligned}\frac{\mathrm{d}L}{\mathrm{d}V}&=L\left(\frac{2}{V}-\frac{R_0}{H}\frac{\mathrm{d}r}{\mathrm{d}V}+\frac{1}{C_L}\frac{\mathrm{d}C_L}{\mathrm{d}V}\right)\\ \frac{\mathrm{d}D}{\mathrm{d}V}&=D\left(\frac{2}{V}-\frac{R_0}{H}\frac{\mathrm{d}r}{\mathrm{d}V}+\frac{1}{C_D}\frac{\mathrm{d}C_D}{\mathrm{d}V}\right)\end{aligned} \tag{14}$$

With the given $\dot{Q}_{\max}$, $q_{\max}$, $n_{\max}$, we can have:

$$\frac{\mathrm{d}\dot{Q}}{\mathrm{d}V}=0,\frac{\mathrm{d}q}{\mathrm{d}V}=0,\frac{\mathrm{d}n}{\mathrm{d}V}=0 \tag{15}$$

Then the first order derivatives of r to V along the boundary of heating rate, dynamic pressure and aerodynamic load constraints are obtained respectively:

$$r'\big|_{\dot{Q}}=\left.\frac{\mathrm{d}r}{\mathrm{d}V}\right|_{\dot{Q}}=\frac{6.3H}{R_0V} \tag{16}$$

$$r'\big|_{n}=\left.\frac{\mathrm{d}r}{\mathrm{d}V}\right|_{n}=\frac{2H}{R_0V} \tag{17}$$

$$r'\big|_{q}=\left.\frac{\mathrm{d}r}{\mathrm{d}V}\right|_{n}=\frac{2H}{R_0V}+\frac{L^2}{L^2+D^2}\frac{1}{C_L}\frac{\mathrm{d}C_L}{\mathrm{d}V}+\frac{D^2}{L^2+D^2}\frac{1}{C_D}\frac{\mathrm{d}C_D}{\mathrm{d}V} \tag{18}$$

The terms contain coefficients C_L and C_D in Eq.(18) are relatively small compared with the first term and Eq.(18) can be written as follow by ignoring the last two terms:

$$r'\big|_{q}=\left.\frac{\mathrm{d}r}{\mathrm{d}V}\right|_{q}=\frac{2H}{R_0V} \tag{19}$$

Integrating Eqs.(16)-(17), and (19), it is found that the heating rate, dynamic pressure and aerodynamic load constraints can be expressed in r-V plane as:

$$\begin{aligned}r&=\frac{6.3H}{R_0}\ln V+C_Q\\ r&=\frac{2H}{R_0}\ln V+C_q\\ r&=\frac{2H}{R_0}\ln V+C_n\end{aligned} \tag{20}$$

From above derivation, we can conclude that when the allowed maximum value of heating rate, dynamic pressure and aerodynamic load are given, the constraint in r-V plane can be expressed as:

$$r=k\ln V+C \tag{21}$$

Where k is valued as $6.3H/R_0$, $2H/R_0$, and $2H/R_0$ for heating rate, dynamic pressure and aerodynamic load respectively. C is integral constant. The same value of k for dynamic pressure and load constraints means these two constraint boundaries are parallel or coincident and only one (the upper one in the r-V plane) of them works. This useful conclusion simplifies the problem significantly.

At the intersection point of constraints, the corresponding velocity is:

$$V = e^{\frac{R_0\left(C_n - C_{\dot{Q}}\right)}{4.3H}} \text{ or } V = e^{\frac{R_0\left(C_q - C_{\dot{Q}}\right)}{4.3H}} \qquad (22)$$

If the trajectory is in the form of Eq.(21), then:

$$\frac{\mathrm{d}r}{\mathrm{d}V} = \frac{k}{V} \qquad (23)$$

With omission of the Coriolis acceleration term in the Eq.(1) we can have:

$$\frac{\mathrm{d}r}{\mathrm{d}V} = \frac{V \sin\gamma}{-D - \sin\gamma / r^2} \qquad (24)$$

The flight path angle can be obtained by:

$$\gamma = \sin^{-1}\left(-\frac{Dk}{V^2 + k/r^2}\right) \qquad (25)$$

If the flight path angle can be predicted during the trajectory planning, we can know whether QEGC is satisfied and then improve the range prediction.

4 Trajectory Planning

The Eq.(21) represented the inherent common of path constraints in r-V plane and is useful for trajectory planning and optimization. Here we take longitudinal trajectory design for example to show the application. It has unique superiority in dealing with path constraints.

The range vehicle has flied:

$$R = -\int \frac{V\mathrm{d}V}{D} \qquad (26)$$

The Eq.(25) indicates that the range can be predicted through designing D=$D(V)$. Since the D-V plane corridor and r-V plane corridor are one to one mapped, we can find an appropriate r=$r(V)$ to satisfy the requirements of range and other performances.

In Fig.1, the dashed line is heating rate constraint; dot-dashed line is load constraint. Re-entry trajectory can be designed as:

$$\begin{aligned} r_1 &= k_1 \ln V + C_1 \\ r_2 &= k_2 \ln V + C_2 \end{aligned} \qquad (27)$$

If the k_1=6.3H/R_0 and k_2=2H/R_0, that means the trajectory is parallel to the constraint boundaries. The intersection velocity is denoted as V_{int}.

Then the trajectory can be adjusted conveniently to satisfy the path constraints when the following conditions hold true:

$$\begin{aligned} C_1 &\geq C_{\dot{Q}} \\ C_2 &\geq C_n \end{aligned} \qquad (28)$$

The value of constants parameters C_1 and C_2 are used to adjust the range. Since the range is monotonous with C_1 and C_2, it will be very fast to find out the right value of these two parameters. There are lots of parameter searching algorithms can be used. This method makes sure that the vehicle can reach any landing site within footprint.

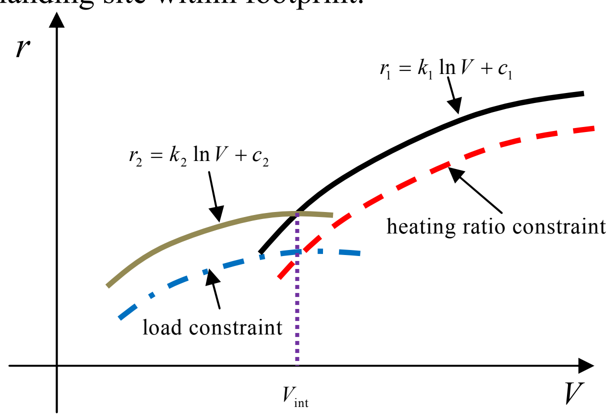

Fig.1 Illustration of constraints for trajectory design

The advantages of this method are as follow:

1) The trajectory can be designed latch on the lower boundary of constraints. So the minimum range can be obtained which enhances capability in solving footprint inner boundary.
2) The designed trajectory is continuous and differentiable (first and second derivatives) and that makes the trajectory tracking much easier.
3) The vehicle flights with constant heating rate, aerodynamic load and dynamic pressure. It conquers the hurt to vehicle structure from continuous changed loads. The reliability such as TPS and vehicle safety are strengthened significantly.

5 Dynamic Inverse Guidance Law

To tracking the designed trajectory, dynamic inverse guidance law is used. It improves the adaptability and robustness of guidance system.

Taking velocity V as independent variable, differentiating the both sides of Eq.(24) with respect to V, we can get:

$$\frac{\mathrm{d}^2 r}{\mathrm{d}V^2} = a + bu \tag{29}$$

$$a = \frac{-1}{Dr^2+\sin\gamma}\left[\frac{(\cos\gamma)^2\left(Vr^2+\frac{\mathrm{d}r}{\mathrm{d}V}\right)(V^2r-1)}{(Dr^2+\sin\gamma)V} - r^2\left(\sin\gamma+\frac{\mathrm{d}D}{\mathrm{d}V}\frac{\mathrm{d}r}{\mathrm{d}V}\right)-\frac{2\sin\gamma}{r}\left(\frac{\mathrm{d}r}{\mathrm{d}V}\right)^2\right]$$

$$b = \frac{\cos\gamma\left(\left(\frac{\mathrm{d}r}{\mathrm{d}V}\right)^3+Vr^2\left(\frac{\mathrm{d}r}{\mathrm{d}V}\right)^2\right)}{r^2V^3\sin^2\gamma}$$

$u = L\cos\sigma$.

The altitude tracking error is denoted as:

$$e = r - r_{\mathrm{ref}} \tag{30}$$

Where r_{ref} is the reference altitude. The first and second derivatives of e with respect to V are:

$$\frac{\mathrm{d}e}{\mathrm{d}V} = \frac{\mathrm{d}r}{\mathrm{d}V} - \frac{\mathrm{d}r_{\mathrm{ref}}}{\mathrm{d}V} \tag{31}$$

$$\frac{\mathrm{d}^2 e}{\mathrm{d}V^2} = \frac{\mathrm{d}^2 r}{\mathrm{d}V^2} - \frac{\mathrm{d}^2 r_{\mathrm{ref}}}{\mathrm{d}V^2} \tag{32}$$

To achieve closed-loop error dynamics in the linear time-invariant form, the tracking altitude error is modeled as a second order system:

$$\frac{\mathrm{d}^2 e}{\mathrm{d}V^2} + 2\varsigma\omega_n\frac{\mathrm{d}e}{\mathrm{d}V} + \omega_n^2 e + k_e\int e\mathrm{d}V = 0 \tag{33}$$

Where k_e is a constant gain. ς and ω_n are damping ratio and nature frequency in velocity domain. Then we can have:

$$\frac{\mathrm{d}^2 r}{\mathrm{d}V^2} = \frac{\mathrm{d}^2 r_{\mathrm{ref}}}{\mathrm{d}V^2} - 2\varsigma\omega_n\frac{\mathrm{d}e}{\mathrm{d}V} - \omega_n^2 e - k_e\int e\mathrm{d}V \tag{34}$$

Using Eq.(29) and (34), the tracking law can be obtained:

$$\sigma = \cos^{-1}\left[\frac{1}{bL}\left(\frac{\mathrm{d}^2 r_{\mathrm{ref}}}{\mathrm{d}V^2} - 2\varsigma\omega_n\frac{\mathrm{d}e}{\mathrm{d}V} - \omega_n^2 e - k_e\int e\mathrm{d}V - a\right)\right] \tag{35}$$

For conveniently scheduling ς and ω_n, we investigate the implicit gain scheduling relationship between the time domain and the velocity domain closed-loop error dynamics and eliminate the effects of dimensionless process. The following two equations are obtained by applying the chain rule:

$$\frac{\mathrm{d}e}{\mathrm{d}t} = \sqrt{R_0 g_0}\frac{\mathrm{d}e}{\mathrm{d}V}\frac{\mathrm{d}V}{\mathrm{d}t} \tag{36}$$

$$\frac{\mathrm{d}^2 e}{\mathrm{d}t^2} = g_0\frac{\mathrm{d}^2 e}{\mathrm{d}V^2}\left(\frac{\mathrm{d}V}{\mathrm{d}t}\right)^2 + g_0\frac{\mathrm{d}e}{\mathrm{d}V}\frac{\mathrm{d}^2 V}{\mathrm{d}t^2} \tag{37}$$

Where $\frac{\mathrm{d}e}{\mathrm{d}t} = \frac{\mathrm{d}r}{\mathrm{d}t} - \frac{\mathrm{d}r_{\mathrm{ref}}}{\mathrm{d}t}, \frac{\mathrm{d}^2 e}{\mathrm{d}t^2} = \frac{\mathrm{d}^2 r}{\mathrm{d}t^2} - \frac{\mathrm{d}^2 r_{\mathrm{ref}}}{\mathrm{d}t^2}$.

In ideal case for the tracking law, k_e =0 in Eq.(33). The closed-loop error dynamics in time domain can be expressed:

$$\frac{\mathrm{d}^2 e}{\mathrm{d}t^2} + 2\varsigma\omega_n\frac{\mathrm{d}e}{\mathrm{d}t} + \omega_n^2 e = 0 \tag{38}$$

Substituting Eq.(36) and (37) into Eq.(38), we can get the dynamics in velocity domain.

$$\frac{\mathrm{d}^2 e}{\mathrm{d}V^2} + 2\overline{\varsigma}\overline{\omega}_n\frac{\mathrm{d}e}{\mathrm{d}V} + \overline{\omega}_n^2 e = 0 \tag{39}$$

Where

$$\overline{\varsigma} = \varsigma + \frac{\frac{\mathrm{d}^2 V}{\mathrm{d}t^2}}{2\omega_n\frac{\mathrm{d}V}{\mathrm{d}t}\sqrt{R_0/g_0}}, \qquad \overline{\omega}_n = \frac{\omega_n\sqrt{R_0/g_0}}{\frac{\mathrm{d}V}{\mathrm{d}t}} \tag{40}$$

Eq.(40) illustrates a complicated relationship between the time domain and the velocity domain for damping ratio and nature frequency. Utilizing this discipline, the $\overline{\varsigma}$ and $\overline{\omega}_n$ can be tuned based on the physical meaning and engineering experience of ς and ω_n which represent typical second order dynamic control system.

6 Simulation

For simulation, the constraint values are set as: $\dot{Q}_{\max} = 794425\mathrm{Wa/s^2}$, $q_{\max}$=14364N/s^2, $n_{\max}$=2.5g,.The angle of attack is predesigned. The re-entry corridor is shown in Fig.2. Because for this condition the aerodynamic load constraint boundary is upper than the dynamic pressure constraint boundary, there are only heating rate and load boundaries work in Fig.2.

The initial conditions are: r=R_0+120km, V=7622.79m/s, θ= -125.0070°, ϕ=-12.2299°, γ=-

1.4377°, ψ=36.8122°. And the terminal condition is: V_f=908.15m/s, r_f=3.0480km.

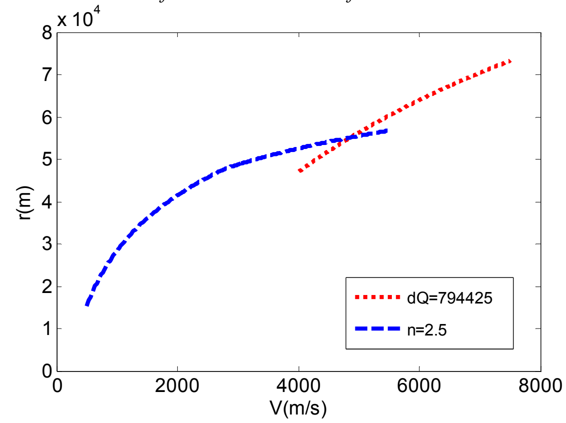

Fig.2 Re-entry corridor

The re-entry trajectory is divided into three phases (as Fig. 4 shows): the initial descent phase, the constant constraint phase and the check phase. In the initial descent phase, from the entry interface to an altitude where aerodynamic lift can provide sufficient control capability, the vehicle falls with a constant bank angle depending on the second phase. The main part of the re-entry trajectory is the constant constraint phase, in which all of the constraints must be observed strictly. The check phase is designed to satisfy the terminal condition.

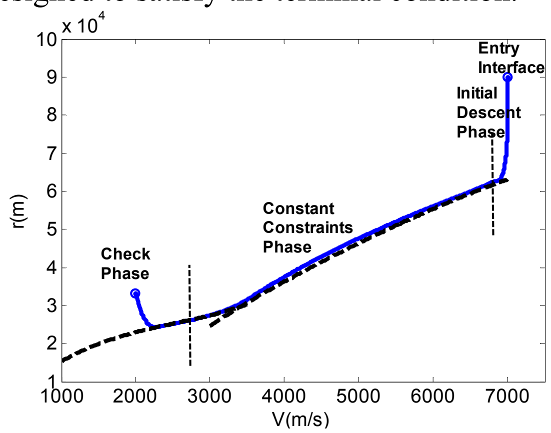

Fig.3 Three phases of the entry trajectory

The designed trajectory is shown with dash line while the tracking trajectory is presented with solid line. The trajectories in r-V plane and are shown in Fig.3 and Fig.4 is the ground track trajectory. And the corresponding bank angle, angle of attack and flight path angle are shown in Fig.5-Fig.7. During initial decent phase, angle of attack is set as 45° and bank angle is set as 40° . It can be found that the dynamic inverse guidance law can track the reference trajectory accurately.

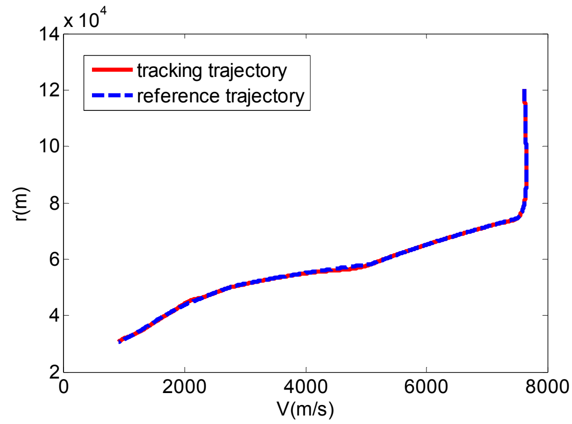

Fig. 4 Trajectory in r-V plane

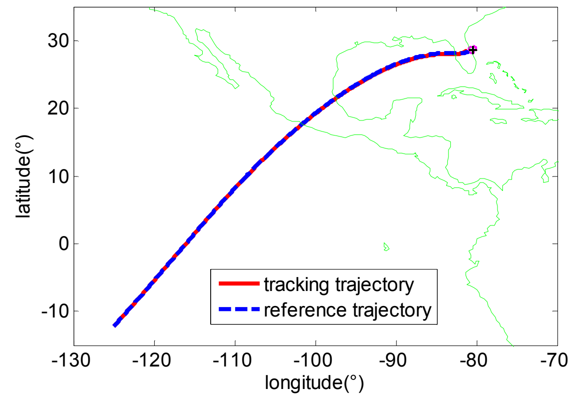

Fig.5 Ground track trajectory

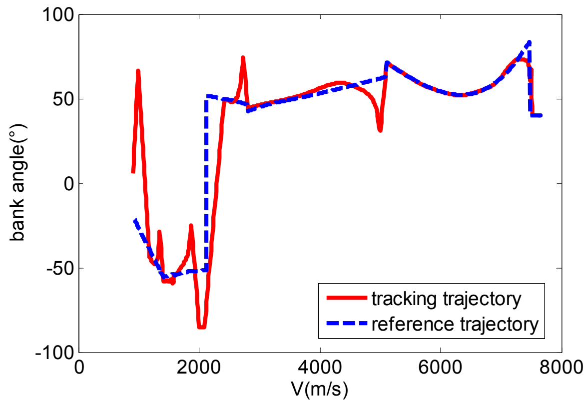

Fig.6 Bank angle

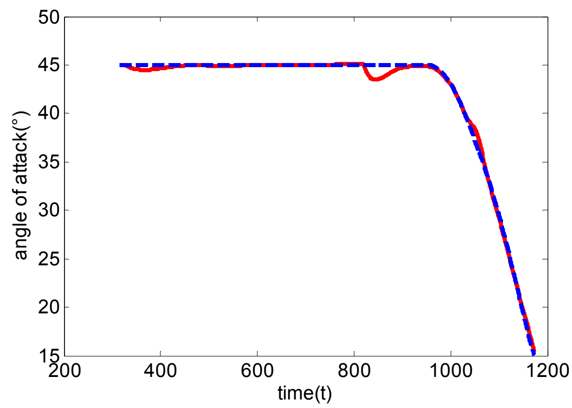

Fig.7 Angle of attack

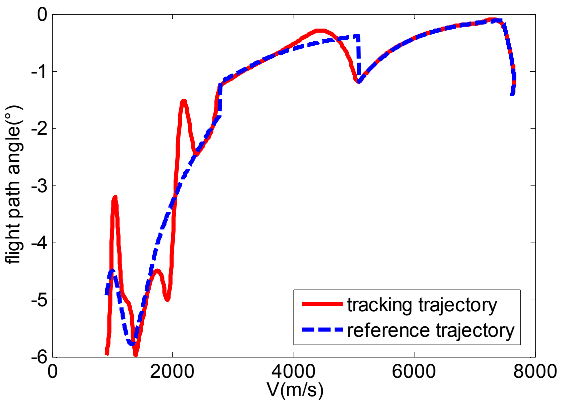

Fig.8 Flight path angle

7 Conclusion

This paper studies an improvement for enhancing guidance system performances in meeting path constraints of re-entry vehicle. The heating rate, aerodynamic load and dynamic pressure path constraints are expressed with a unified formula in *r*-*V* plane. Based on the unified formula a new trajectory planning method is developed and used in shaping the reference profile in *r*-*V* plane to better fit the re-entry corridor. This method has fewer parameters and can satisfy path constraints easily. Dynamic inverse guidance law is designed to track the trajectory. The proposed approach can simplify re-entry trajectory planning and tracking problems.

References

[1] Hanson J M, Jones R E. Test results for entry guidance methods for space vehicles. *Journal of Guidance, Control, and Dynamic*, Vol. 27, No. 6, pp 960-966, 2004.
[2] Xue S B, Lu P. Constrained predictor-corrector entry guidance. *Journal of Guidance, Control, and Dynamic*, Vol. 33, No. 4, pp 1273-1281, 2010.
[3] Harpold J C, Graves C A. Shuttle Entry Guidance. *Journal of the Astronautical Science*, Vol. 27, No. 3, pp 239-268, 1979.
[4] Spratlin K M. An Adaptive Numeric Predictor-corrector Guidance Algorithm for Atmospheric Entry Vehicle. Cambridge: Massachusetts Institute of Technology, 2001.
[5] Zimmerman C, Dukeman G A, Hanson J M. Automated Method to Compute Orbital Reentry Trajectories with Heating Constraints. *Journal of Guidance, Control, and Dynamics*, Vol. 26, No. 4, pp 523-529, 2003.
[6] Shen Z J, Lu P. Onboard Generation of Three-Dimensional Constrained Entry Trajectories. *Journal of Guidance, Control, and Dynamics*, Vol. 26, No. 1, pp 111-121, 2003.
[7] Vinh N X, Busemann A, Culp R D. Hypersonic and Planetary Entry Flight Mechanics. Ann Arbor, Michigan: Univ. of Michigan Press, 1980.
[8] Regan F J, Satya M. *Dynamics of Atmospheric Reentry*, Washington, DC: AIAA, 1993.

Copyright Statement